PERGAMON

International Journal of Heat and Mass Transfer 42 (1999) 1945–1956

International Journal of HEAT and MASS TRANSFER

Heat transfer and friction correlation for compact louvered fin-and-tube heat exchangers

C.-C. Wang[a,*], C.-J. Lee[b], C.-T. Chang[b], S.-P. Lin[a]

[a] *Energy and Resources Laboratories, Industrial Technology Research Institute, Hsinchu, Taiwan, Republic of China*
[b] *Department of Mechanical Engineering, Yuan-Ze University, Chung Li, Taiwan, Republic of China*

Received 25 December 1997; in final form 28 August 1998

Abstract

General heat transfer and friction correlations for louver fin geometry having round tube configuration were proposed in the present study. A total of 49 samples of louvered fin-and-tube heat exchangers with different geometrical parameters, including louver pitch, louver height, longitudinal tube pitch, transverse tube pitch, tube diameter, and fin pitch were used to develop the correlations. The proposed correlation describes 95.5% of the Coburn j and 90.8% of the friction factors within $\pm 15\%$. © 1998 Elsevier Science Ltd. All rights reserved.

Key words: Louver fin; Heat transfer; Friction; Correlation; Heat exchanger

Nomenclature

A area [m^2]
A_c minimum free-flow area [m^2]
A_f fin surface area [m^2]
A_o total surface area [m^2]
A_t external tube surface area [m^2]
C heat capacity rate [W K^{-1}]
C_1, C_2, C_3, C_4 correlation parameters, dimensionless
c_p specific heat at constant pressure [J kg^{-1} K^{-1}]
D_c fin collar outside diameter $D_o + 2\delta_f$ [mm]
D_i inside tube diameter [mm]
D_h hydraulic diameter $4A_cL/A_o$ [mm]
D_o outside diameter of round tube [mm]
f friction factor, dimensionless
Fp fin pitch [mm]
$F1$, $F2$, $F3$, $F4$, $F5$, $F6$, $F7$, $F8$, $F9$ correlation parameters, dimensionless
G_c mass flux of the air based on the minimum flow area [kg m^{-2} s^{-1}]
h heat transfer coefficient [W m^{-2} K^{-1}]
j $Nu/(RePr^{1/3})$, the Colburn factor, dimensionless
$J1$, $J2$, $J3$, $J4$, $J5$, $J6$, $J7$, $J8$ correlation parameters, dimensionless
k thermal conductivity [W m^{-1} K^{-1}]
K_c abrupt contraction pressure-loss coefficient, dimensionless
K_e abrupt expansion pressure-loss coefficient, dimensionless
L_h louver height [mm]
L_p major louver pitch [mm]
N number of longitudinal tube rows, dimensionless
NTU UA/C_{min}, number of transfer units, dimensionless
ΔP pressure drop [Pa]
P_l longitudinal tube pitch [mm]
Pr Prandtl number dimensionless
P_t transverse tube pitch [mm]
$\dot{Q}$ heat transfer rate [W]
$\dot{Q}_{max}$ $C_{min}(T_{water,in} - T_{air,in})$, the maximum possible heat transfer rate [W]
r radius of the tube diameter, including collar fin thickness [mm]
Re_{Dc} Reynolds number based on tube collar diameter, dimensionless
R_{eq} equivalent radius for circular fin [mm]
T temperature [°C]
U overall heat transfer coefficient [W m^{-2} K^{-1}]
V velocity [m s^{-1}]
X_L $\sqrt{(P_t/2)^2 + P_l^2}/2$, geometric parameter [mm]

* Corresponding author: D500 ERL/ITRI, Bldg. 64, 195–6 Section 4, Chung Hsing Road, Chutung, 310, Hsinchu, Taiwan, Republic of China. Tel.: 00 886 3 5916294; fax: 00 886 3 5820250; e-mail: ccwang@erl.itri.org.tw

0017–9310/99/$ - see front matter
PII: S0017–9310(98)00302–0

X_M $P_t/2$, geometric parameter [mm].

Greek symbols

δ thickness [mm]
ε $\dot{Q}/\dot{Q}_{max}$, heat exchanger effectiveness, dimensionless
θ louver angle, degree
δ_f fin thickness [mm]
δ_w wall thickness [mm]
η fin efficiency, dimensionless
η_0 surface efficiency, dimensionless
μ dynamic viscosity of fluid [kg m^{-1} s^{-1}]
ρ mass density of fluid [kg m^{-3}]
σ contraction ratio of cross-sectional area, dimensionless.

Subscripts

air air side
i tube side
1 inlet
2 outlet
f fin surface
min minimum value
max maximum value
o total surface
w wall.

1. Introduction

Finned tube heat exchangers are widely used in a variety of applications such as air-conditioning, refrigeration and in the process industry. Generally, the heat exchangers consist of a plurality of spaced parallel tubes through which a heat transfer medium such as water, oil or refrigerant is forced to flow while a second heat transfer fluid like air is directed across the tubes. For most practical applications, airside thermal resistance is roughly 5 to 10 times that of the refrigerant side. Consequently, enhanced surfaces are often employed to effectively improve the overall performance of the fin-and-tube heat exchanger. One of the very popular enhanced surfaces is the interrupted surface. This is because the interrupted surfaces can provide higher average heat transfer coefficients owing to periodical renewal of the development of boundary layer. The most common interrupted surfaces are offset strip and louver fin. The louvered fin pattern is more beneficial when produced in large quantities since it can be manufactured by high-speed production techniques. There are a couple of variants of louver fin heat exchangers as combined with the tubes. For automotive application, such as radiators, condensers and evaporators, the louver fins are generally brazed (or soldered, mechanically expanded) to a flat, extruded tube, with a cross section of several independent passages, and formed into a serpentine or a parallel flow geometry (Fig. 1a). For applications to residential air-conditioning systems, the fin-and-tube heat exchangers are consisted of mechanically or hydraulically expanded round tubes in a block of parallel continuous fins as indicated in Fig. 1b. During the past few decades, there had been numbers of experimental works devoted to the louver fin geometry for Fig. 1a configuration. Recently, a general heat transfer correlation that compiled more than 91 samples was reported by Chang and Wang [1].

Conversely, for louver fin having round tube configuration (Fig. 1b), general design correlation for the airside performance is not available. This is because the airside performances are usually considered proprietary. There are several related investigations by Wang and his co-workers [2–6] who provided valuable information about the louver fin pattern. However, their test results were limited to specific louver fin patterns and an attempt to construct a universal correlation based on the previous published results is not yet accomplished. Furthermore, as pointed out by Wang et al. [3], the heat transfer and friction characteristics of louver fin-and-tube heat exchangers (Fig. 1b) are quite different from those of Fig. 1a. This is because complex interactions between the fin and round tube and variable length of louver are shown. Therefore the main objective of this study is to construct a generalized heat transfer and friction correlation based on the previous investigations [2–7].

2. The data bank

An attempt has been made to collect data from a wide range of geometric dimensions. However, the airside performance for enhanced surfaces is generally proprietary for the industry and manufacturers. As a result, the databank is based on the previous works by the present authors [2–7]. In Table 1, a complete list of various louver fin has been given and the relevant geometric parameters are shown. Detailed description of the present louver fins and the terminology of louver fin is shown in Fig. 2. A total of 49 samples are used for the development of correlations. The data are from Wang et al. [3] (17 samples, Fig. 2, Type I), Wang et al. [4] (14 samples, Fig. 2, Type 2), Wang et al. [5] (6 samples, Fig. 2, Type III), Wang et al. [5] (4 samples, Fig. 1, Type IV), Chi et al. [6] (4 samples, Fig. 2, Type V) and Wang [7] (4 samples, Fig. 2, type VI). As shown in Fig. 3, the circuitry of the present test samples are all pure cross-flow configuration.

3. Data reduction of heat transfer coefficient and frictions factors

The detailed reduction method for the test data had been described by several previous studies [3–6] and will not be repeated here. The heat transfer coefficients were

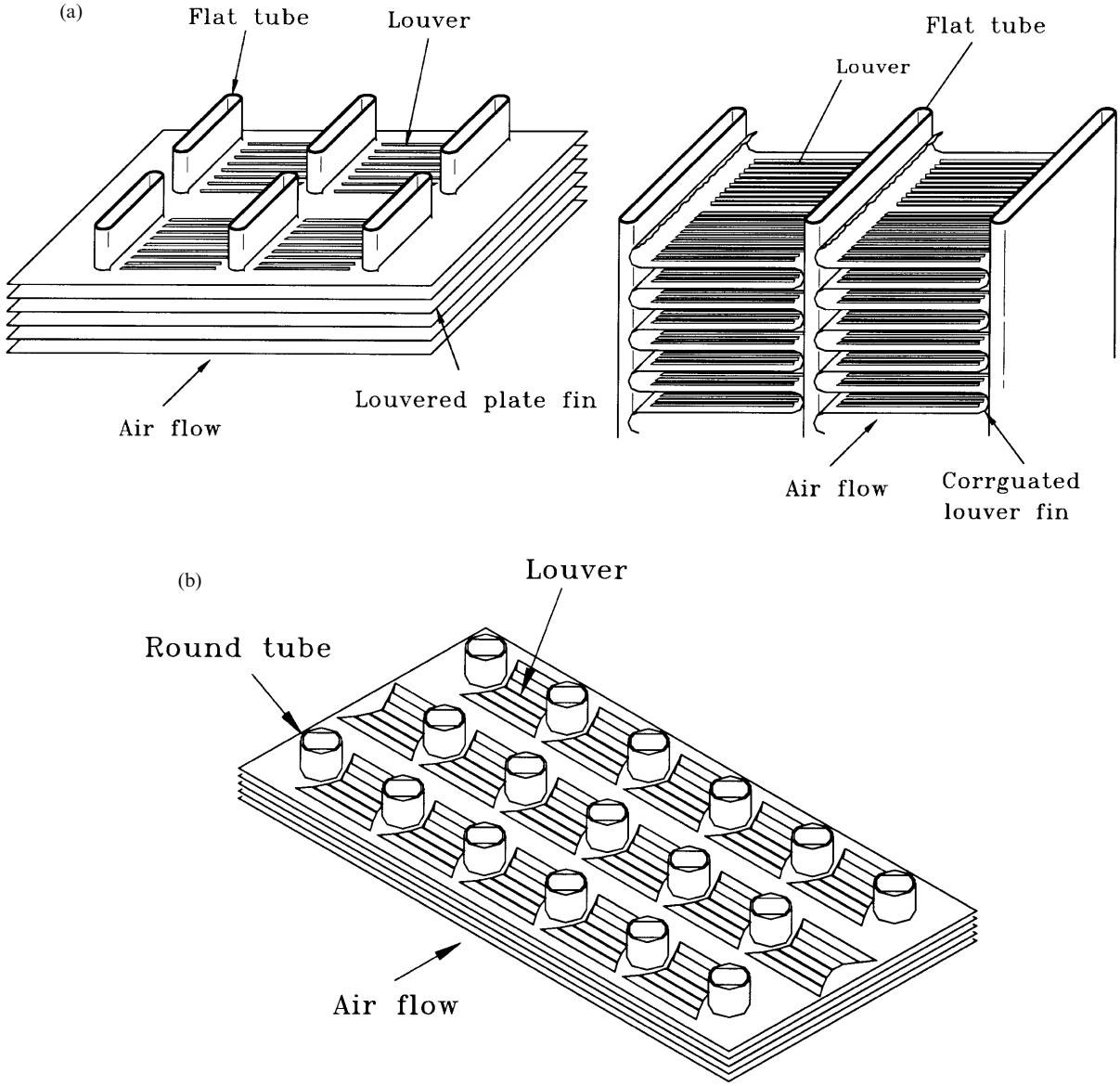

Fig. 1. (a) Typical louver fin geometry with flat tube configuration. (b) Typical louver fin geometry with round tube configuration.

reduced using the ε–NTU methods. It is noted that the number of tube rows for the present test samples ranges from 1 to 6. In some of the previous investigations [2–4], the authors used the relationships for cross flow having both sides unmixed to reduce their heat transfer coefficients. The corresponding ε–NTU relationship [8] is

$$\varepsilon = 1-\exp[NTU^{0.22}\cdot\{\exp(-C^*\cdot NTU^{0.78})-1\}/C^*] \quad (1)$$

Equation (1) is an approximation of cross-flow configuration having infinite numbers of tube rows. Typical louvered fin-and-tube heat exchangers generally consist of less than six rows, therefore the effect of the number of tube rows should be taken into account (N is finite). The corresponding ε–NTU relationships, taking from the ESDU [9], for 1–4 row configuration are tabulated in Table 2. For a number of tube rows greater than 4, ESDU [9] suggests an unmixed/unmixed flow arrangement having $N = \infty$ as the approximation, i.e. equation (1). Figure 4 shows a plot of ε vs NTU for $C^* = 0.4$ and 1.0. As seen in the figure, the approximation by equation (1) gives very good agreement with those of $N = \infty$. For $NTU < 2$ and $N > 1$, the differences in effectiveness are negligible. However, for $NTU > 3$, the effectiveness for $N = \infty$ exceeds $N = 1$ by more than 0.1. Therefore unacceptable

Table 1
Geometric dimensions of the sample louver fin heat exchangers

No.	Type	Fin pitch [mm]	D_c [mm]	P_t [mm]	P_l [mm]	Louver height [mm]	Major louver pitch [mm]	Row no.
1	I	1.50	10.42	25.4	19.05	1.4	2.4	1
2	I	2.05	10.42	25.4	19.05	1.4	2.4	1
3	I	1.50	10.42	25.4	19.05	1.4	2.4	2
4	I	2.05	10.42	25.4	19.05	1.4	2.4	2
5	I	1.30	10.42	25.4	19.05	1.4	2.4	3
6	I	1.81	10.42	25.4	19.05	1.4	2.4	3
7	I	1.29	10.42	25.4	19.05	1.4	2.4	4
8	I	1.49	10.42	25.4	19.05	1.4	2.4	4
9	I	1.79	10.42	25.4	19.05	1.4	2.4	4
10	I	2.08	10.42	25.4	19.05	1.4	2.4	4
11	I	1.51	10.42	25.4	19.05	1.4	2.4	6
12	I	2.07	10.42	25.4	19.05	1.4	2.4	6
13	I	1.50	8.71	25.4	19.05	1.4	2.4	1
14	I	2.07	8.71	25.4	19.05	1.4	2.4	1
15	I	1.52	8.71	25.4	19.05	1.4	2.4	2
16	I	2.08	8.71	25.4	19.05	1.4	2.4	2
17	I	1.53	8.71	25.4	19.05	1.4	2.4	4
18	II	1.50	10.42	25.4	19.05	0.9	3.75	1
19	II	2.05	10.42	25.4	19.05	0.9	3.75	1
20	II	1.52	10.42	25.4	19.05	0.9	3.75	2
21	II	2.06	10.42	25.4	19.05	0.9	3.75	2
22	II	1.53	10.42	25.4	19.05	0.9	3.75	4
23	II	2.06	10.42	25.4	19.05	0.9	3.75	4
24	II	1.51	10.42	25.4	19.05	0.9	3.75	6
25	II	2.08	10.42	25.4	19.05	0.9	3.75	6
26	II	1.51	8.71	25.4	19.05	0.9	3.75	1
27	II	2.09	8.71	25.4	19.05	0.9	3.75	1
28	II	1.51	8.71	25.4	19.05	0.9	3.75	2
29	II	2.09	8.71	25.4	19.05	0.9	3.75	2
30	II	1.51	8.71	25.4	19.05	0.9	3.75	4
31	II	2.10	8.71	25.4	19.05	0.9	3.75	4
32	III	1.21	10.33	25.4	19.05	1.07	2.35	1
33	III	1.82	10.33	25.4	19.05	1.07	2.35	1
34	III	2.49	10.33	25.4	19.05	1.07	2.35	1
35	III	1.21	10.33	25.4	19.05	1.07	2.35	2
36	III	1.78	10.33	25.4	19.05	1.07	2.35	2
37	III	2.42	10.33	25.4	19.05	1.07	2.35	2
38	IV	1.21	10.33	25.4	22	1.07	2	1
39	IV	2.47	10.33	25.4	22	1.07	2	1
40	IV	1.21	10.33	25.4	22	1.07	2	2
41	IV	2.49	10.33	25.4	22	1.07	2	2
42	V	1.66	7.53	21	12.7	0.79	1.7	2
43	V	1.22	7.53	21	12.7	0.79	1.7	2
44	V	1.73	7.53	21	12.7	0.79	1.7	4
45	V	1.22	7.53	21	12.7	0.79	1.7	4
46	VI	1.20	6.93	17.7	13.6	1.4	1.7	1
47	VI	1.99	6.93	17.7	13.6	1.4	1.7	1
48	VI	1.23	6.93	17.7	13.6	1.4	1.7	2
49	VI	1.98	6.93	17.7	13.6	1.4	1.7	2

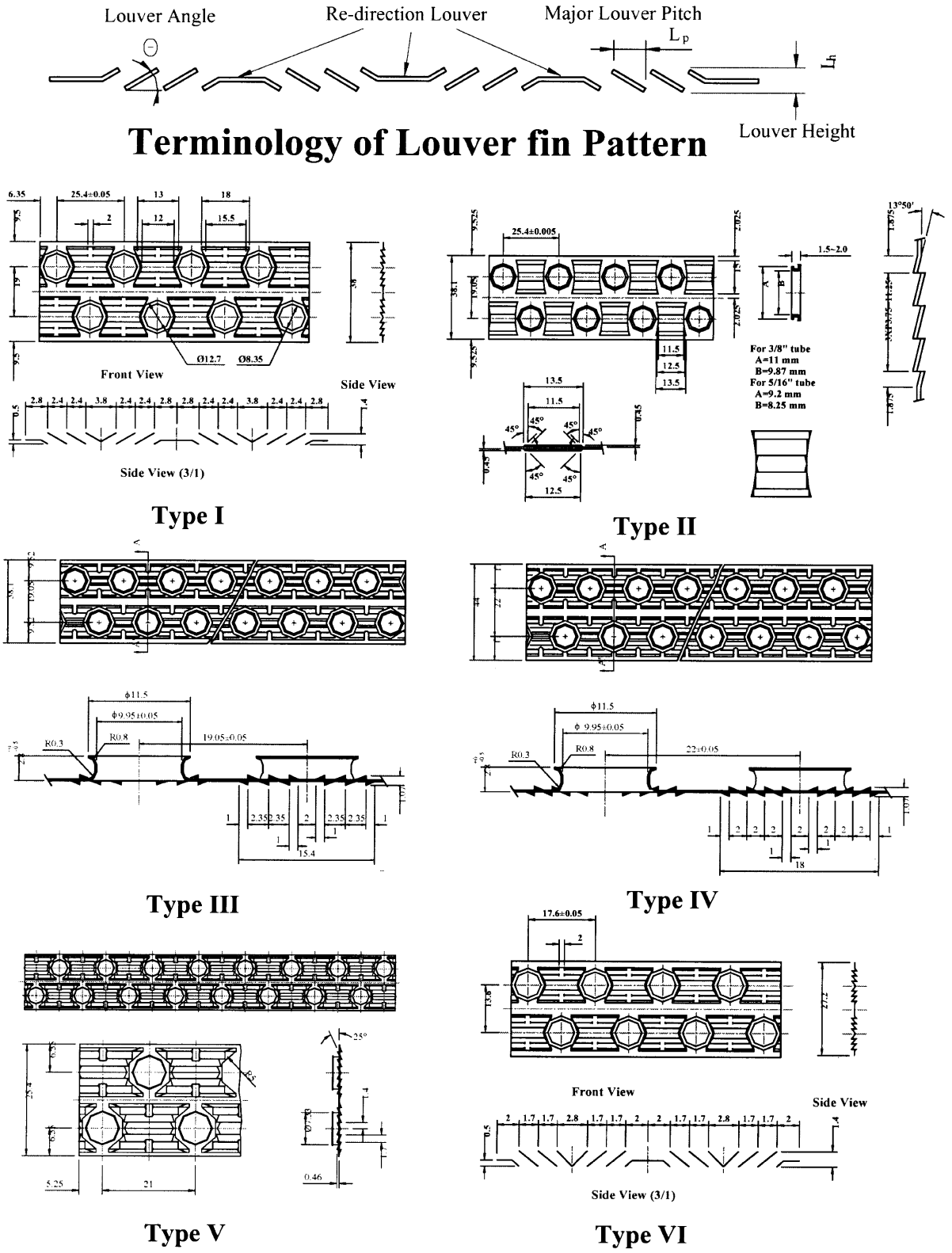

Fig. 2. Details of the present louver fin configuration.

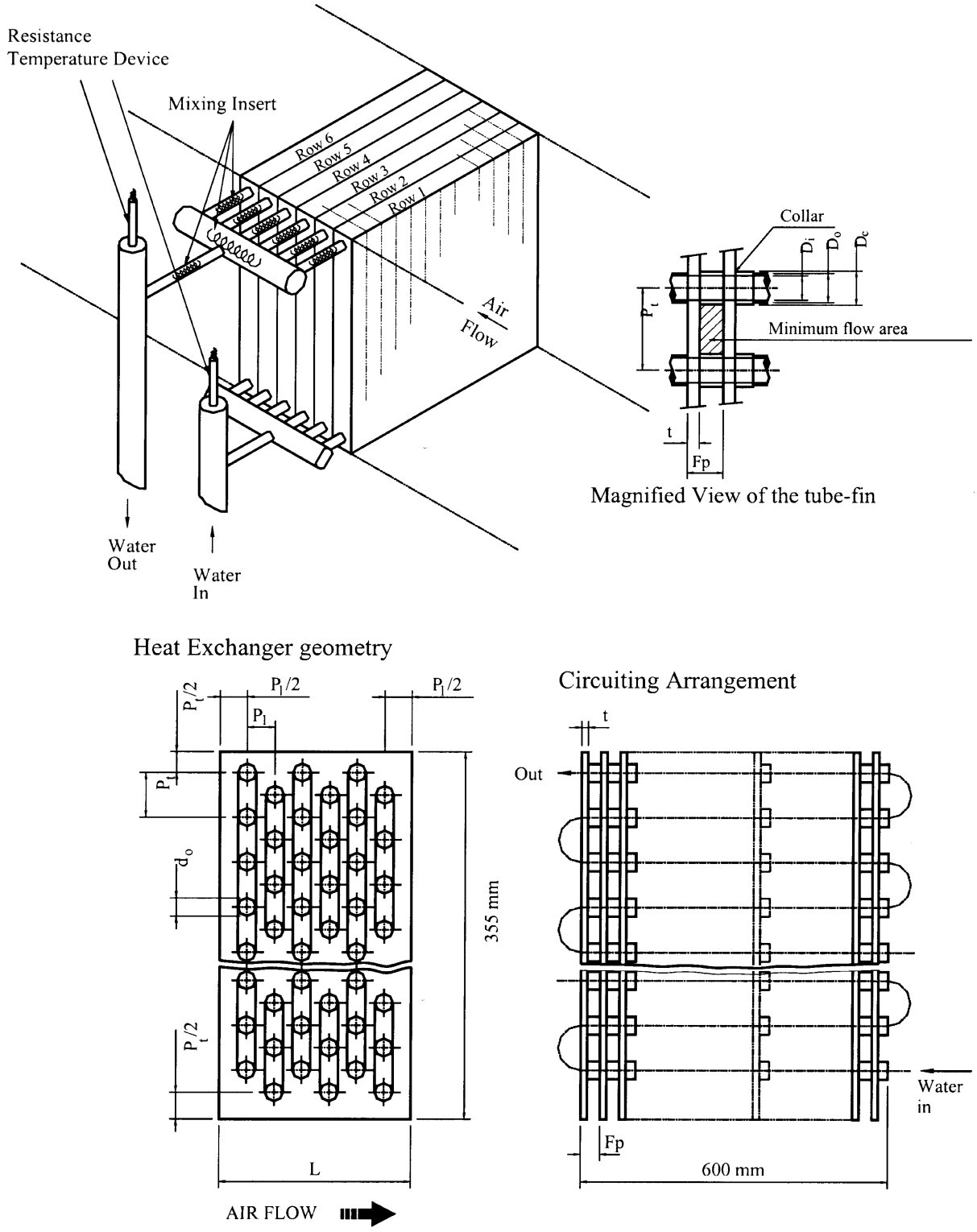

Fig. 3. Schematic of the construction of test samples.

Table 2
ε–NTU relationship for cross-flow configuration

Number of tube row	Side of C_{min}	Formula
1	Air	$\varepsilon = \frac{1}{C^*}[1-e^{-C^*(1-e^{-NTU})}]$
	Tube	$\varepsilon = 1-e^{-(1-e^{-NTU\cdot C^*})/C^*}$
2	Air	$\varepsilon = \frac{1}{C^*}[1-e^{-2KC^*}(1+C^*K^2)]$ $K = 1-e^{-NTU/2}$
	Tube	$\varepsilon = 1-e^{-2K/C^*}\left(1+\frac{K^2}{C^*}\right)$ $K = 1-e^{-NTU\cdot C^*/2}$
3	Air	$\varepsilon = \frac{1}{C^*}\left[1-e^{-3KC^*}\left(1+C^*K^2(3-K)+\frac{3(C^*)^2K^4}{2}\right)\right]$ $K = 1-e^{-NTU/3}$
	Tube	$\varepsilon = 1-e^{-3K/C^*}\left(1+\frac{K^2(3-K)}{C^*}+\frac{3K^4}{2(C^*)^2}\right)$ $K = 1-e^{-NTU\cdot C^*/3}$
4	Air	$\varepsilon = \frac{1}{C^*}\left[1-e^{-4KC^*}\left(1+C^*K^2(6-4K+K^2)+4(C^*)^2K^4(2-K)+\frac{8(C^*)^3K^6}{3}\right)\right]$ $K = 1-e^{-NTU/4}$
	Tube	$\varepsilon = 1-e^{-4K/C^*}\left(1+\frac{K^2(6-4K+K^2)}{C^*}+\frac{4K^4(2-K)}{(C^*)^2}+\frac{8K^6}{3(C^*)^3}\right)$ $K = 1-e^{-NTU\cdot C^*/4}$
∞	—	$\varepsilon = 1-e^{[NTU^{0.22}\cdot\{e(-C^*\cdot NTU^{0.78})-1\}/C^*]}$ Note: unmixed–unmixed formula

results of reduced heat transfer coefficients may occur when applying equation (1) to reduce the heat transfer coefficients. Fortunately, the NTU values for previous study having $N = 1$ are generally less than 2.0 which corresponds to a maximum difference of 4% for the reduced results of heat transfer coefficients. However, for consistency of data reduction, we had re-reduced all the test data based on the relationships of Table 2. It should be further emphasized here that the use of correct ε–NTU relationships should be carefully examined before applying the present heat transfer correlation to size/rate a heat exchanger.

For rating of a fin-and-tube heat exchanger using the present heat transfer correlation, the following procedures should be followed:

(1) Obtain the heat transfer coefficients, h_0, from the present correlation.
(2) Calculate the fin efficiency using the Schmidt approximation [10],

$$\eta = \frac{\tanh(mr\phi)}{mr\phi} \tag{2}$$

where

$$m = \sqrt{\frac{2h_o}{k_f\delta_f}} \tag{3}$$

$$\phi = \left(\frac{R_{eq}}{r}-1\right)[1+0.35\ln(R_{eq}/r)] \tag{4}$$

For staggered tube layout

$$\frac{R_{eq}}{r} = 1.27\frac{X_M}{r}\left(\frac{X_L}{X_M}-0.3\right)^{1/2} \tag{5}$$

and for an inline layout, or 1-row coil,

$$\frac{R_{eq}}{r} = 1.28\frac{X_M}{r}\left(\frac{X_L}{X_M}-0.2\right)^{1/2} \tag{6}$$

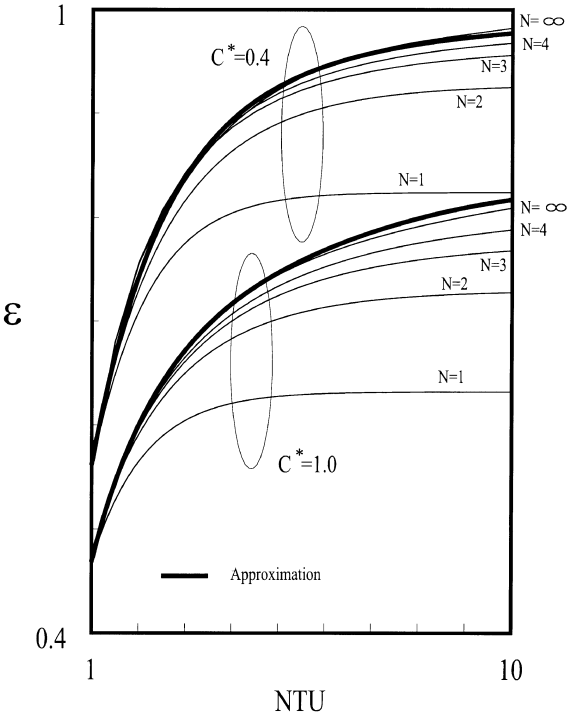

Fig. 4. The ε–NTU relationship accounting for the number of tube rows.

(3) Calculate the surface effectiveness from the fin efficiency η,

$$\eta_o = 1 - \frac{A_f}{A_o}(1-\eta) \tag{7}$$

(4) Obtain the in-tube heat transfer coefficients, h_i, from appropriate correlations. For single-phase fluid within a smooth tube, h_i can be evaluated from the Gnielinski [11] semi-empirical correlation:

$$h_i = \left(\frac{k}{D}\right)_i \frac{(Re_i - 1000)Pr(f_i/2)}{1 + 12.7\sqrt{f_i/2}(Pr^{2/3}-1)} \tag{8}$$

where

$$f_i = (1.58\ln(Re_i) - 3.28)^{-2} \tag{9}$$

$$Re_i = \rho V D_i/\mu \tag{10}$$

(5) Calculate the overall heat transfer resistance from the following relationship,

$$\frac{1}{UA} = \frac{1}{\eta_o h_o A_o} + \frac{\delta_w}{k_w A_w} + \frac{1}{h_i A_i} \tag{11}$$

(6) Obtain the NTU from

$$NTU \equiv UA/C_{min} \tag{12}$$

(7) Use the appropriate ε–NTU relationships to calculate the effectiveness ε according to the arrangement of circuitry. For a flow arrangement similar to Fig. 2, the relationships shown in Table 2 are applicable.

(8) Obtain the heat transfer rate by

$$\dot{Q} = \varepsilon \dot{Q}_{max} \tag{13}$$

The core friction of the heat exchanger is calculated from the pressure drop equation proposed by Kays and London [12]. The present Fanning friction factors had included the entrance and exit pressure loss, and are expressed as below:

$$f = \frac{A_c \rho_1}{A_o \rho_m}\left[\frac{2\Delta P}{G_c^2 \rho_1} - (1+\sigma^2)\left(\frac{\rho_1}{\rho_2} - 1\right)\right] \tag{14}$$

where A_0 and A_c stand for the total surface area and the flow cross-sectional area, respectively. The term, σ, is the ratio of the minimum flow area to frontal area.

Notice that some of the previous investigations [2–4] had excluded the entrance and exit pressure loss coefficients in the Fanning friction factors, i.e.

$$f = \frac{A_c}{A_o}\frac{\rho_m}{\rho_1}\left[\frac{2\rho_1 \Delta P}{G_c^2} - (K_c + 1 - \sigma^2) - 2\left(\frac{\rho_1}{\rho_2} - 1\right) + (1 - \sigma^2 - K_e)\frac{\rho_1}{\rho_2}\right] \tag{15}$$

The entrance and exit loss coefficients K_c and K_e are adapted from Figs 14–26 of McQuiston and Parker [8]. However, for the present configuration, periodic contraction and expansion may occur for each row. As a result, it is difficult to differentiate the form drag and fin friction from the total pressure drop. As a result, the friction factors were re-reduced using equation (14). It is very important to note that equation (14) should be used to calculate the friction factors when applying the proposed friction correlation.

4. Construction of the correlation

Figure 5 shows the distribution of j factor for all tests. Note that the Reynolds number is based on the collar diameter, D_c. As seen, considerable scattering of airside performance is observed owing to significant differences in the geometrical parameters for the louver fins. Furthermore, for louver fin having re-direction louver, smaller fin pitch, and larger number of tube row, the Coburn j factors experienced a 'level-off' phenomenon at low Reynolds number. This phenomenon had been explained by several previous works [3, 13]. More interestingly, Type II did not reveal this kind of phenomenon [4]. Consequently, it is appropriate to divide the range to correlate the test data.

The test results for friction factors are shown in Fig. 6.

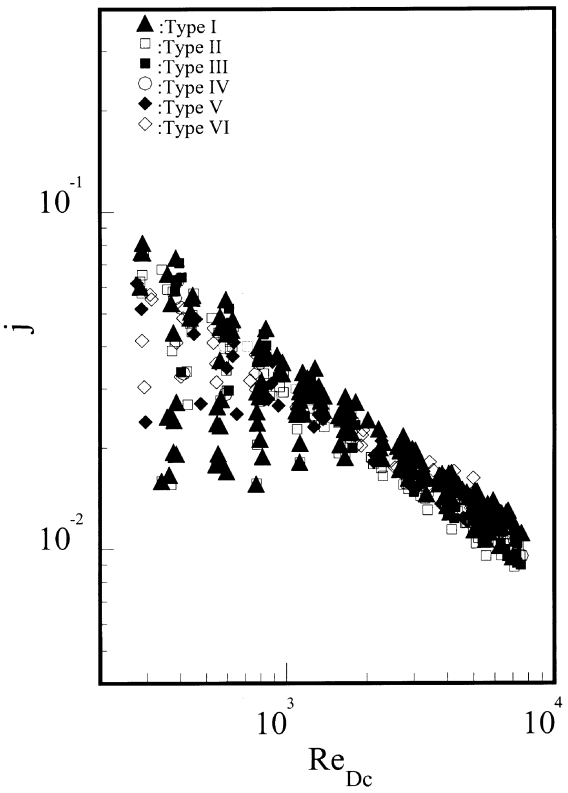

Fig. 5. The Coburn j factors vs Re_{Dc} for the present samples.

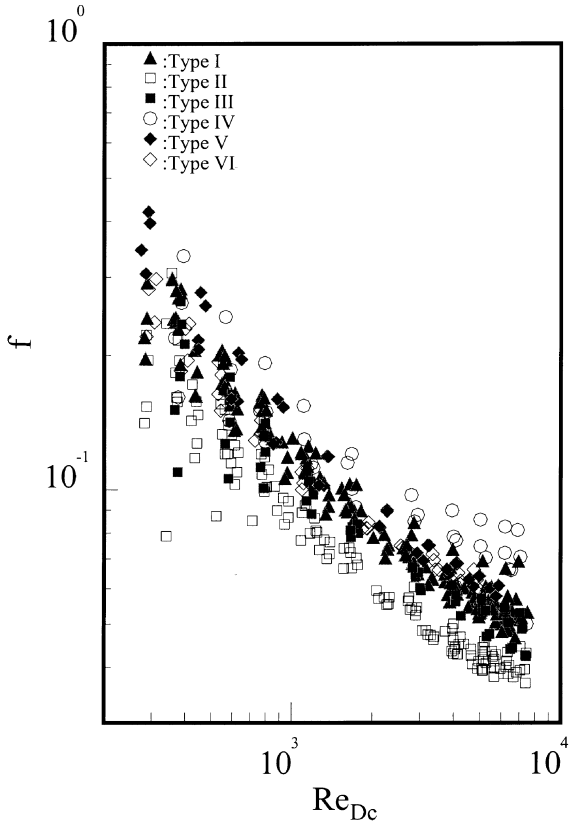

Fig. 6. Friction factors, f, vs Re_{Dc} for the present samples.

For $Re_{Dc} = 6000$, the friction factors for Type IV are approximately two times higher than those of Type II. In general, Type II louver fin shows the lowest airside performance due to its smallest louver angle of 13.5°.

It is obvious from the Figs 5 and 6 that no single curve can be expected to describe the complex behaviors of both j and f factors. In addition, the 'level-off' phenomenon for the Coburn j factors makes the problem even more complicated. Attempts are made to correlate the present test results using a multiple regression technique. The basic forms of the correlations are:

$$j = C_1 Re_{Dc}^{C_2} \tag{16}$$

$$f = C_3 Re_{Dc}^{C_4} \tag{17}$$

It is assumed that the parameters of C_1, C_2, C_3 and C_4 depend on the physical dimensions of the heat exchanger. A separate multiple linear regression was carried out to determine the exponents, C_2 and C_4 of the test data. The determinations of C_1 and C_3 are analogous to those of C_2 and C_4. After a trial and error process, the final equations for the j factors are given as follows:

For $Re_{Dc} < 1000$

$$j = 14.3117 Re_{Dc}^{J1} \left(\frac{F_p}{D_c}\right)^{J2} \left(\frac{L_h}{L_p}\right)^{J3} \left(\frac{F_p}{P_l}\right)^{J4} \left(\frac{P_l}{P_t}\right)^{-1.724} \tag{18}$$

where

$$J1 = -0.991 - 0.1055 \left(\frac{P_l}{P_t}\right)^{3.1} \log_e\left(\frac{L_h}{L_p}\right) \tag{19}$$

$$J2 = -0.7344 + 2.1059 \left(\frac{N^{0.55}}{\log_e(Re_{Dc}) - 3.2}\right) \tag{20}$$

$$J3 = 0.08485 \left(\frac{P_l}{P_t}\right)^{-4.4} N^{-0.68} \tag{21}$$

$$J4 = -0.1741 \log_e(N) \tag{22}$$

For $Re_{Dc} \geqslant 1000$

$$j = 1.1373 Re_{Dc}^{J5} \left(\frac{F_p}{P_l}\right)^{J6} \left(\frac{L_h}{L_p}\right)^{J7} \left(\frac{P_l}{P_t}\right)^{J8} (N)^{0.3545} \tag{23}$$

where

$$J5 = -0.6027+0.02593\left(\frac{P_l}{D_h}\right)^{0.52}(N)^{-0.5}\log_e\left(\frac{L_h}{L_p}\right) \quad (24)$$

$$J6 = -0.4776+0.40774\left(\frac{N^{0.7}}{\log_e(Re_{Dc})-4.4}\right) \quad (25)$$

$$J7 = -0.58655\left(\frac{F_p}{D_h}\right)^{2.3}\left(\frac{P_l}{P_t}\right)^{-1.6}N^{-0.65} \quad (26)$$

$$J8 = 0.0814(\log_e(Re_{Dc})-3) \quad (27)$$

$$D_h = \frac{4A_c}{L} \quad (28)$$

Notice that equation (18) is valid for $Re_{Dc} < 1000$, and equation (23) is applicable to $Re_{Dc} \geqslant 1000$.

The correlation of friction factor is given as:
For $N = 1$,

$$f = 0.00317Re_{Dc}^{F1}\left(\frac{F_p}{P_l}\right)^{F2}\left(\frac{D_h}{D_c}\right)^{F3}\left(\frac{L_h}{L_p}\right)^{F4}\left(\log_e\left(\frac{A_o}{A_t}\right)\right)^{-6.0483} \quad (29)$$

$$F1 = 0.1691+4.4118\left(\frac{F_p}{P_l}\right)^{-0.3}\left(\frac{L_h}{L_p}\right)^{-2}\left(\log_e\left(\frac{P_l}{P_t}\right)\right)\left(\frac{F_p}{P_t}\right)^{3} \quad (30)$$

$$F2 = -2.6642-14.3809\left(\frac{1}{\log_e(Re_{Dc})}\right) \quad (31)$$

$$F3 = -0.6816\log_e\left(\frac{F_p}{P_l}\right) \quad (32)$$

$$F4 = 6.4668\left(\frac{F_p}{P_t}\right)^{1.7}\log_e\left(\frac{A_o}{A_t}\right) \quad (33)$$

$N > 1$

$$f = 0.06393Re_{Dc}^{F5}\left(\frac{F_p}{D_c}\right)^{F6}\left(\frac{D_h}{D_c}\right)^{F7}\left(\frac{L_h}{L_p}\right)^{F8} \times N^{F9}(\log_e(Re_{Dc})-4.0)^{-1.093} \quad (34)$$

$$F5 = 0.1395-0.0101\left(\frac{F_p}{P_l}\right)^{0.58}\left(\frac{L_h}{L_p}\right)^{-2}\left(\log_e\left(\frac{A_o}{A_t}\right)\right)\left(\frac{P_l}{P_t}\right)^{1.9} \quad (35)$$

$$F6 = -6.4367\left(\frac{1}{\log_e(Re_{Dc})}\right) \quad (36)$$

$$F7 = 0.07191\log_e(Re_{Dc}) \quad (37)$$

$$F8 = -2.0585\left(\frac{F_p}{P_t}\right)^{1.67}\log_e(Re_{Dc}) \quad (38)$$

$$F9 = 0.1036\left(\log_e\left(\frac{P_l}{P_t}\right)\right) \quad (39)$$

Figure 7 shows the comparisons of the experimental data with equations (18) and (23). The present heat transfer correlation can describe 95.5% of the j factors within $\pm 15\%$ while the proposed friction correlation, equations (29) and (34) can correlate 90.8% of the test data within $\pm 15\%$. Detailed comparisons of the proposed correlations are tabulated in Table 3. As seen, the present heat transfer correlation gives a mean deviation of 5.72% whereas the proposed friction correlation shows a 8.73% mean deviation.

5. Conclusions

A generalized heat transfer and friction correlation for louver fin geometry is proposed in the present study. A

Table 3
Comparison of the proposed correlation with the experimental data

Deviation	$\pm 10\%$	$\pm 15\%$	$\pm 20\%$	$\pm 25\%$	Mean deviation	Average deviation
j	84.9%	95.5%	99.4%	99.6%	5.72%	0.27%
f	65.6%	90.8%	96.3%	98.7%	8.73%	−0.55%

$$\text{Average deviation} = \frac{1}{M}\left(\sum_1^M \frac{j_{pred}-j_{exp}}{j_{exp}}\right)\times 100\%.$$

$$\text{Mean deviation} = \frac{1}{M}\left(\sum_1^M \frac{|j_{pred}-j_{exp}|}{j_{exp}}\right)\times 100\%.$$

M: number of data points.

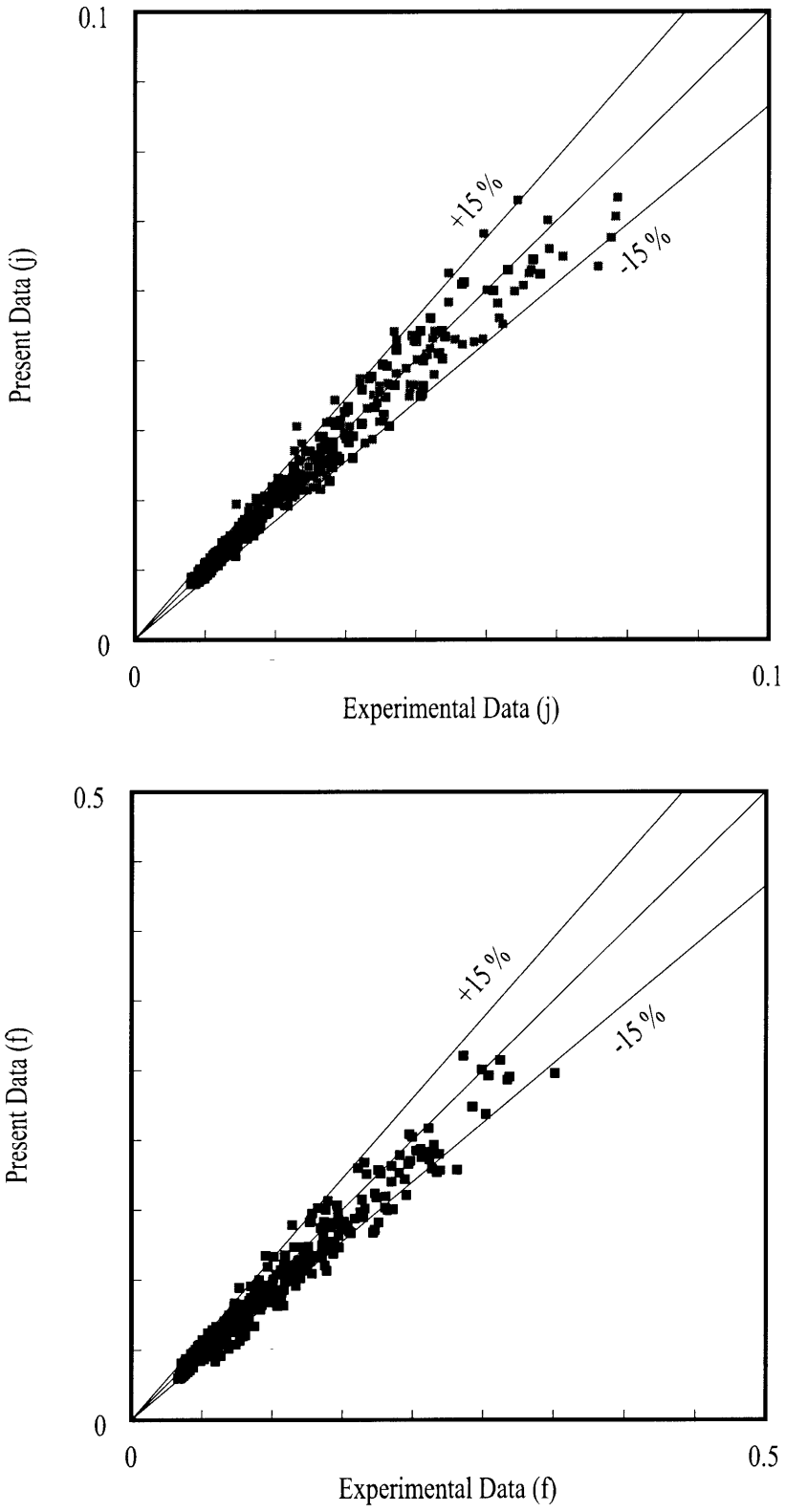

Fig. 7. Comparisons of the present heat transfer and friction correlations with the experimental data.

total of 49 fin-and-tube heat exchangers having louver fins are used in the regression analysis. The proposed heat transfer correlation can describe 95.5% of the test data within $\pm 15\%$ with a mean deviation of 5.72% while the proposed friction correlation can describe 90.8% of the results within $\pm 15\%$ with a mean deviation of 8.73%.

Acknowledgements

The authors would like to express gratitude for the Energy Research and Development Foundation funding from the Energy Commission of the Ministry of Economic Affairs, Taiwan, which provides support for the current study.

References

[1] Y.J. Chang, C.C. Wang, A generalized heat transfer correlation for louver fin geometry, Int. J. Heat Mass Transfer 40 (3) (1998) 533–544.

[2] W.R. Chang, C.C. Wang, W.C. Tsi, R.J. Shyu, Air side performance of louver fin heat exchanger, in: Proceedings of the Fourth ASME/JSME Thermal Engineering Joint Conference, vol. 4, 1995, pp. 367–372.

[3] C.C. Wang, Y.P. Chang, K.U. Chi, Y.J. Chang, An experimental study of heat transfer and friction characteristics of typical louver fin and tube heat exchangers, Int. J. Heat Mass Transfer 41 (4–5) (1998) 817–822.

[4] C.C. Wang, Y.P. Chang, K.U. Chi, Y.J. Chang, A study of non-redirection louver fin-and-tube heat exchangers, in: Proceedings of the Institute of Mechanical Engineering, Part C, J. Mech. Eng. Sci. 212 (1998) 1–14.

[5] C.C. Wang, C.J. Lee, C.T. Chang, Some aspects of the fin-and-tube heat exchangers: with and without louvers, J. Enhanced Heat Transfer 1998, in press.

[6] K.U. Chi, C.C. Wang, Y.J. Chang, Y.P. Chang, A comparison study of compact plate fin-and-tube exchanger, ASHRAE Trans. 1998, in press.

[7] C.C. Wang, ERL louver fin test data, unpublished data for four louver fins, 1997.

[8] F.C. McQuiston, J.D. Parker, Heating, Ventilating, and Air-conditioning, 4th ed., John Wiley and Sons Inc., 1994, Chap. 14, p. 571.

[9] ESDU 86018, Engineering Science Data Unit 86018 with Amendment A, ESDU International plc, London, July 1991, pp. 92–107.

[10] ThE. Schmidt, Heat transfer calculations for extended surfaces, Refrig. Eng. April (1949) 351–357.

[11] V. Gnielinski, New equation for heat and mass transfer in turbulent pipe and channel flow, Int. Chem. Engng. 16 (1976) 359–368.

[12] W.M. Kays, A.L. London, Compact Heat Exchangers, 3rd ed., McGraw-Hill, New York, 1984.

[13] C.C. Wang, Y.J. Chang, Y.C. Hsieh, Y.T. Lin, Sensible heat and friction characteristics of plate fin-and-tube heat exchangers having plane fins, Int. J. Refrig. 19 (4) (1996) 223–230.